MOLECULAR IMAGING AND BIOLOGY

Mol Imaging Biol (2019) 21:368–374
DOI: 10.1007/s11307-018-1223-x

Published Online: 21 June 2018

RESEARCH ARTICLE

Associations Between [^{18}F]FDG-PET and Complex Histopathological Parameters Including Tumor Cell Count and Expression of KI 67, EGFR, VEGF, HIF-1α, and p53 in Head and Neck Squamous Cell Carcinoma

Alexey Surov,[1] Hans Jonas Meyer,[1] Anne-Kathrin Höhn,[2] Karsten Winter,[3] Osama Sabri,[4] Sandra Purz[4]

[1]*Department of Diagnostic and Interventional Radiology, University Hospital of Leipzig, Liebigstrasse 20, 04103, Leipzig, Germany*
[2]*Department of Pathology, University Hospital of Leipzig, Liebigstrasse 20, 04103, Leipzig, Germany*
[3]*Institute of Anatomy, University Hospital of Leipzig, Liebigstrasse 20, 04103, Leipzig, Germany*
[4]*Department of Nuclear Medicine, University Hospital of Leipzig, Liebigstraße 18, 04103, Leipzig, Germany*

Abstract

Purpose: Head and neck squamous cell carcinoma (HNSCC) is one of common cancers worldwide. Positron emission tomography (PET) with 2-deoxy-2-[^{18}F]fluoro-D-glucose ([^{18}F]FDG) is increasingly used for diagnosing and staging, as well as for monitoring of treatment of HNSCC. PET parameters like maximum and mean standard uptake values (SUV_{max}, SUV_{mean}) can predict the behavior of HNSCC. The purpose of this study was to analyze possible associations between these PET parameters and clinically relevant histopathological features in patients with HNSCC.

Procedures: Overall, 22 patients, mean age, 55.2 ± 11.0 years, with different HNSCC were acquired. Low grade (G1/2) tumors were diagnosed in 10 cases (45 %) and high grade (G3) tumor in 12 (55 %) patients. In all cases, whole body PET was performed. For this study, the following specimen stainings were performed: MIB-1 staining (KI 67 expression), epidermal growth factor receptor (EGFR), vascular endothelial growth factor (VEGF), tumor suppressor protein p53, hypoxia-inducible factor (HIF)-1α, and human papilloma virus (p16 expression). All stained specimens were digitalized and analyzed by using the ImageJ software 1.48v. Spearman's correlation coefficient (ρ) was used to analyze associations between investigated parameters. P values <0.05 were taken to indicate statistical significance.

Results: P16-negative tumors showed statistically significant higher SUV_{max} ($\rho = 0.006$) and SUV_{mean} values ($\rho = 0.002$) in comparison to p16-positive carcinomas. No significant differences were identified in the analyzed parameters between poorly and moderately/well-differentiated tumors. In overall sample, there were no statistically significant correlations between the [^{18}F]FDG-PET and histopathological parameters. Also, in G1/2 tumors, no significant correlations were identified. In G3 carcinomas, cell count correlated statistical significant with SUV_{max} ($\rho = 0.580$, $P = 0.048$) and SUV_{mean} ($\rho = 0.587$, $P = 0.045$).

Correspondence to: Alexey Surov; *e-mail:* alex.surow@medizin.uni-halle.de

Conclusion: Associations between [^{18}F]FDG-PET parameters and different histopathological features in HNSCC depend significantly on tumor grading. In G1/2 carcinomas, there were no significant correlations between [^{18}F]FDG-PET parameters and histopathology. In G3 lesions, SUV_{max} and SUV_{mean} reflect tumor cellularity.

Key words: SUV, PET, HNSCC, KI 67, VEGF, EGFR, HIF-1α, p53

Introduction

Head and neck squamous cell carcinoma (HNSCC) is one of common cancers worldwide [1]. Positron emission tomography (PET) with 2-deoxy-2-[^{18}F]fluoro-D-glucose ([^{18}F]FDG-PET) is increasingly used for diagnosing and staging, as well as for monitoring of treatment of HNSCC [2, 3]. It has been shown that [^{18}F]FDG-PET provides additional accuracy and is superior to x-ray computed tomography (CT) or magnetic resonance imaging (MRI) or ultrasound alone in the detection of cervical lymph node status of oral cavity squamous cell carcinoma [2, 3]. Nowadays, combination of [^{18}F]FDG-PET and CT or MRI is integrated in the work-up of head and neck cancer patients [4–7]. So Ryu et al. reported that [^{18}F]FDG-PET/CT staging was significantly more sensitive and accurate than conventional workups staging including physical examination, endoscopy, CT, and/or MRI and provided important staging information improving management and prognostic stratification in HNSCC [8].

According to the literature, [^{18}F]FDG-PET parameters can predict tumor stage and behavior of HNSCC. For example, Haerle et al. showed that metabolic tumor activity correlated with T stage of HNSCC [9]. Other authors confirmed this finding and suggested that [^{18}F]FDG-PET parameters like standardized uptake values (SUV_{max}, SUV_{mean}, and SUV_{peak}), metabolic tumor volume (MTV), and total lesion glycolysis (TLG) were associated with pathologically advanced T stage (T3/T4) [10]. Furthermore, Li et al. reported that SUV values were related to grade of differentiation of HNSCC, namely well-differentiated tumors showed significantly lower SUVs than poorly differentiated lesions [11].

[^{18}F]FDG-PET parameters are also associated with clinical outcome in HNSCC. So far, in the study of Abgral et al., MTV was identified as an independent prognostic value of event-free survival and overall survival in patients with HNSCC [12]. According to Kim et al., patients with high metabolic tumor burden were associated with higher distant metastasis rates, translating into worse survival [13]. Finally, [^{18}F]FDG-PET parameters can also predict treatment success in HNSCC. For instance, Kitagawa et al. showed that SUV values were useful in predicting the response to treatment [14]. Furthermore, Wong et al. showed that MTV and/or TLG can be used as predictive biomarkers for ultimate response to subsequent chemoradiotherapy [15].

The reported data suggest that [^{18}F]FDG-PET parameters may be associated with several histopathological findings in HNSCC. Therefore, the purpose of this study was to analyze possible associations between [^{18}F]FDG-PET parameters and clinically relevant histopathological features in patients with HNSCC.

Material and Methods

This prospective study was approved by the institutional review board.

Patients

For this study, 22 patients, 6 (27 %) women and 16 (73 %) men, mean age, 55.2 ± 11.0 years, range 24–77 years, with different HNSCC were acquired (Table 1). G1/2 tumors were diagnosed in 10 cases (45 %) and high grade (G3) tumor in 12 (55 %) patients.

Imaging

PET/CT In all 22 patients, a [^{18}F]FDG-PET/CT (Siemens Biograph 16, Siemens Medical Solutions, Erlangen, Germany) was performed from the skull to the upper thigh after a fasting period of at least 6 h. Application of [^{18}F]FDG was performed intravenously with a body weight-adapted dose (4 MBq/kg, range 168–427 MBq, mean ± std: 281 ± 62.2 MBq). PET/CT image acquisition started on average 76 min (range 60–90 min) after application of [^{18}F]FDG. Low-dose CT was used for attenuation correction of the PET-Data.

The acquired PET/CT datasets were evaluated by a board-certified nuclear medicine and a board-certified radiologist with substantial PET/CT experience in oncological image interpretation. PET/CT image analysis was performed on the dedicated workstation of Hermes Medical Solutions, Sweden. For each tumor, maximum and mean SUV (SUV_{max}; SUV_{mean}) were determined on PET images. Prior to this, tumor margins of the HNSCC were identified on diagnostic CT images and fused PET/CT images and a polygonal volume of interest (VOI), that include the entire lesion in the axial, sagittal, and coronal planes, was placed in the PET dataset (SUV_{max} threshold 40 %) (see Fig. 1).

Table 1. Characteristics of the patients/tumors involved into the study

N	Sex	Age	Tumor site	T stage	N stage	M stage	Grading
1	f	33	Tongue	3	0	0	2
2	m	62	Larynx	3	3	0	3
3	m	55	Tonsil	3	2	0	3
4	m	56	Hypopharynx	3	1	0	3
5	f	58	Oropharynx	1	2	0	3
6	m	24	Oral cavity	4	2	0	2
7	m	64	Oral cavity	2	1	0	3
8	m	57	Tonsil	2	2	0	3
9	m	44	Larynx	4	0	0	3
10	f	77	Epipharynx	4	1	1	3
11	m	59	Tonsil	3	1	0	2
12	m	53	Larynx	4	2	0	3
13	m	64	Hypopharynx	4	2	0	2
14	m	61	Oropharynx	4	2	0	2
15	m	58	Oropharynx	2	2	0	2
16	f	60	Oropharynx	4	2	0	3
17	m	55	Tonsil	3	2	0	2
18	m	54	Oral cavity	4	2	0	2
19	f	65	Tonsil	2	2	0	3
20	m	50	Tonsil	2	2	0	3
21	m	48	Hypopharynx	2	2	0	2
22	f	58	Tongue	4	2	0	1

Histopathological Findings

In all cases, the diagnosis was confirmed histopathologically by tumor biopsy. The biopsy specimens were deparaffinized, rehydrated, and cut into 5-µm slices. Thereafter, the histological slices were stained by MIB 1 monoclonal antibody (DakoCytomation, Glostrup, Denmark), epidermal growth factor receptor (EGFR, EMERGO Europe, clone 111.6, dilution 1:30), vascular endothelial growth factor (VEGF, EMERGO Europe, clone VG1, dilution 1:20), tumor suppressor protein p53 (DakoCytomation, Glostrup, Denmark; clone DO-7, dilution 1:100), hypoxia-inducible factor (HIF)-1α (Biocare Medical, 60 Berry Dr Pacheco, CA 94553; clone EP1215Y, dilution 1:100), and human papilloma virus (p16 expression, Cintec Histology, Roche, Germany) according to previous descriptions [4, 16–20].

On the next step, all stained specimens were digitalized by using the Pannoramic microscope scanner (Pannoramic SCAN, 3DHISTECH Ltd., Budapest, Hungary) with Carl Zeiss objectives up to ×41 bright field magnification by default. In the used bottom-up approach, the whole sample is acquired at high resolution. Low magnification representations are automatically obtained. *Via* Pannoramic Viewer 1.15.4 (open source software, 3D HISTECH Ltd., Budapest, Hungary), slides were evaluated and three captures with a magnification of ×200 were extracted of each sample.

Further analyses of the digitalized histopathological images were performed by using the ImageJ software 1.48v (National Institutes of Health Image program) with a Windows operating system [4, 21, 22]. Tumor proliferation index KI 67 was estimated on MIB 1-stained specimens as a ratio: (number of stained nuclei ÷ number of all nuclei) × 100 %. For the analysis, the area with the highest number of positive tumor nuclei was selected (Fig. 2a). Tumor cell count as a number of all nuclei was estimated on MIB 1-stained specimens as reported previously [4, 21]. The analyzed tumors were divided into p16 positive and p16 negative based on p16 expression [16].

Furthermore, expression of EGFR, VEGF, HIF-1α, and p53 (Fig. 2b–e) was estimated as a sum of stained areas (μm^2) according to previous description [23].

Statistical Analysis

Statistical analysis was performed using SPSS package (IBM SPSS Statistics for Windows, version 22.0, Armonk, NY: IBM corporation). Collected data were evaluated by means of descriptive statistics.

Spearman's correlation coefficient (ρ) was used to analyze associations between investigated parameters. *P* values <0.05 were taken to indicate statistical significance.

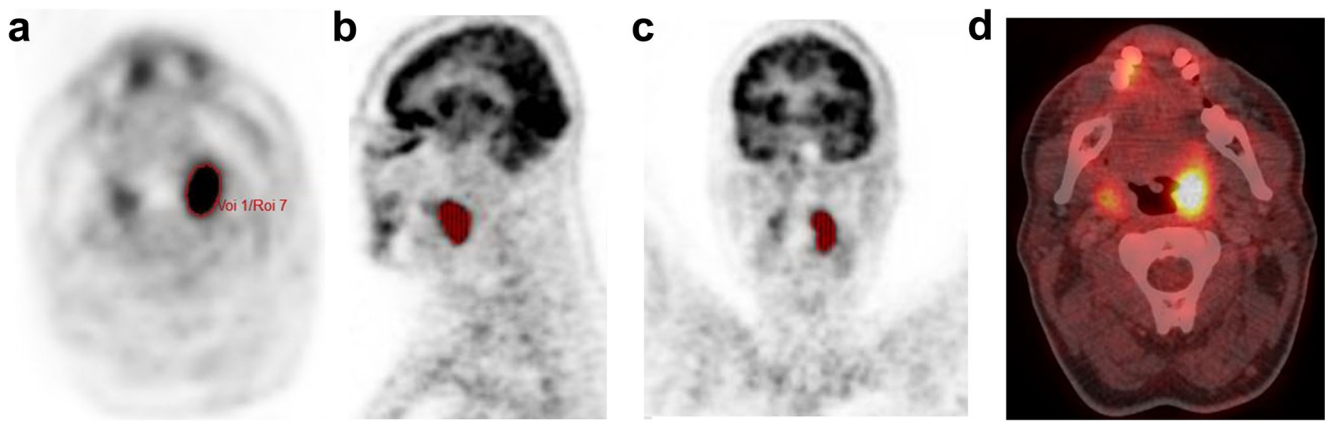

Fig. 1 [^{18}F]FDG-PET/CT findings in a patient with HNSCC of the left oropharynx. Lesion with polygonal volume of interest (VOI) in the **a** axial, **b** sagittal, and **c** coronal planes. SUV_{max} = 10.6, SUV_{mean} = 6.2. **d** Fused [^{18}F]FDG-PET/CT image demonstration of the metabolic active HNSCC of the left oropharynx (arrow).

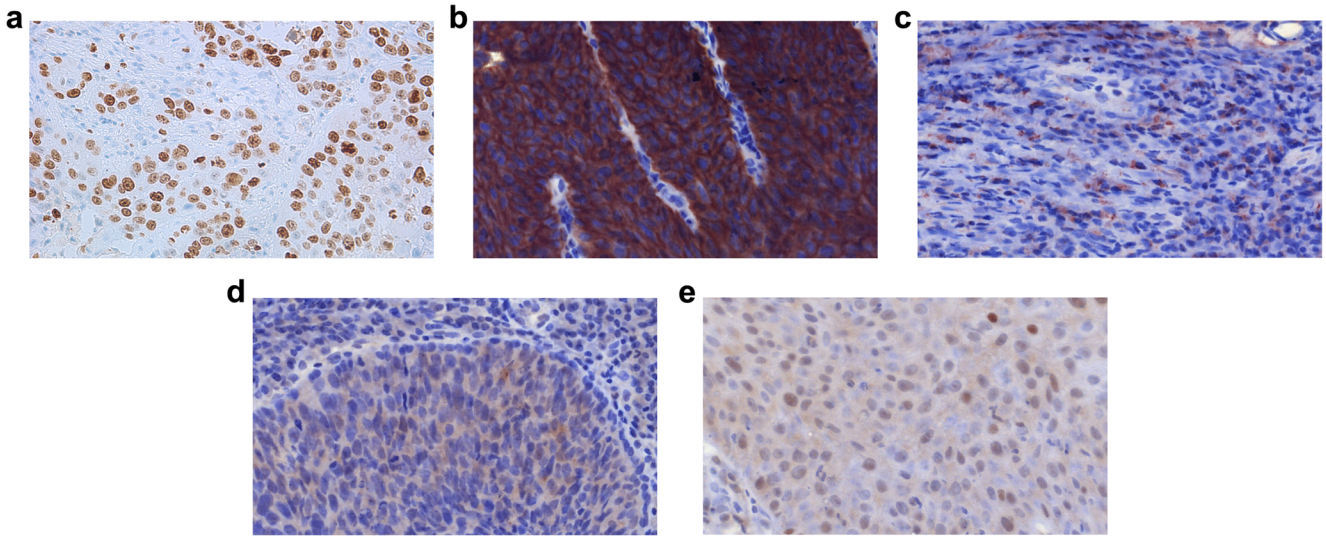

Fig. 2 Histopathological features of the tumor. **a** MIB-1 staining. KI 67 index is 35 %. Cell count is 244. **b** EGFR staining. Stained area is 110,834 μm^2. **c** VEGF staining. Stained area is 9202 μm^2. **d** HIF-1α staining. Stained area is 15,006 μm^2. **e** p53 staining. Stained area is 10,467 μm^2.

Results

A complete overview of the results including mean values, standard deviation, and ranges is shown in Table 2. The tumors showed a wide spectrum of proliferation activity ranging from 24 to 97 %, mean value, 66 %. Furthermore, the lesions had different expression values of VEGF, EGFR, HIF-1α, and p53 (Table 2). In 14 patients (64 %), p16 positive and in 8 patients (36 %), p16-negative tumors were diagnosed.

P16-negative tumors showed statistically significant higher SUV_{max} (19.07 ± 4.70 *vs* 12.48 ± 3.38, $P = 0.006$) and SUV_{mean} values (11.10 ± 3.34 *vs* 7.33 ± 2.04, $P = 0.002$) in comparison to p16-positive carcinomas (Fig. 3). No significant differences were identified in the analyzed parameters between poorly and moderately/well-differentiated tumors (SUV_{max} 14.13 ± 4.20 *vs* 15.59 ± 4.72, $P = 0.60$; SUV_{mean} 8.49 ± 3.49 *vs* 8.90 ± 2.97, $P = 0.78$).

In overall sample, there were no statistically significant correlations between the FDG-PET and histopathological parameters (Table 3). Also in G1/2 tumors, no significant correlations were identified. Only HIF-1α tended to correlate with SUV_{max} ($p = -0.624$, $P = 0.054$) and SUV_{mean} ($p = -0.564$, $P = 0.09$) (Table 3). In G3 carcinomas, however, cell count correlated statistical significant with SUV_{max} ($p = 0.580$, $P = 0.048$) and SUV_{mean} ($p = 0.587$, $P = 0.045$) (Table 3).

Table 2. Estimated parameters of HNSCC

Parameters	M ± SD	Median	Range
SUV_{max}	14.3 ± 5.1	14.8	5.9–24.1
SUV_{mean}	8.4 ± 3.1	8.3	3.7–14.9
Cell count	199 ± 78	186	97–403
Ki 67, %	66 ± 22.4	64	24–97
EGFR expression, μm^2	85,069 ± 62,154	56,610	8755–245,157
VEGF expression, μm^2	15,584 ± 17,549	9294	0–51,745
HIF-1α expression, μm^2	24,597 ± 22,496	13,552	452–67,894
p53 expression, μm^2	29,987 ± 29,159	27,925	188–86,688

Discussion

The present study investigated associations between different [^{18}F]FDG-PET parameters and histopathological findings in HNSCC.

According to the literature, several biomarkers play an important role in HNSCC [24–26]. Especially, proliferation index KI 67, epidermal growth factor receptor (EGFR), tumor suppressor protein p53, vascular endothelial growth factor (VEGF), human papilloma virus (p16 expression), and hypoxia-inducible factor (HIF)-1α were highlighted [26–32]. It has been shown that high expression of KI 67 correlated with tumoral aggressiveness and worse prognosis in patients with HNSCC [24, 25]. Another biomarker, EGFR is involved in the regulation of many cellular responses, including cell proliferation, apoptosis, and cellular differentiation [27]. Some studies indicated that EGFR expression represents a good prognostic parameter in HNSCC [27, 28]. Furthermore, p53 regulates the activity of pathways, which lead variously to cell cycle arrest, senescence, or apoptosis following exposure of cells to endogenous or exogenous cellular stresses [29]. VEGF overexpression has been reported as a poor predictor for patients with head and neck cancer [30]. Human papilloma virus is common among HNSCC and has been reported as an independent prognostic factor [31]. Finally, HIF-1α characterizes cellular responses to hypoxic stress [32]. Overexpression of HIF-1α was significantly associated with increase of mortality risk and worse prognosis of HNSCC [32]. Therefore, the question, if

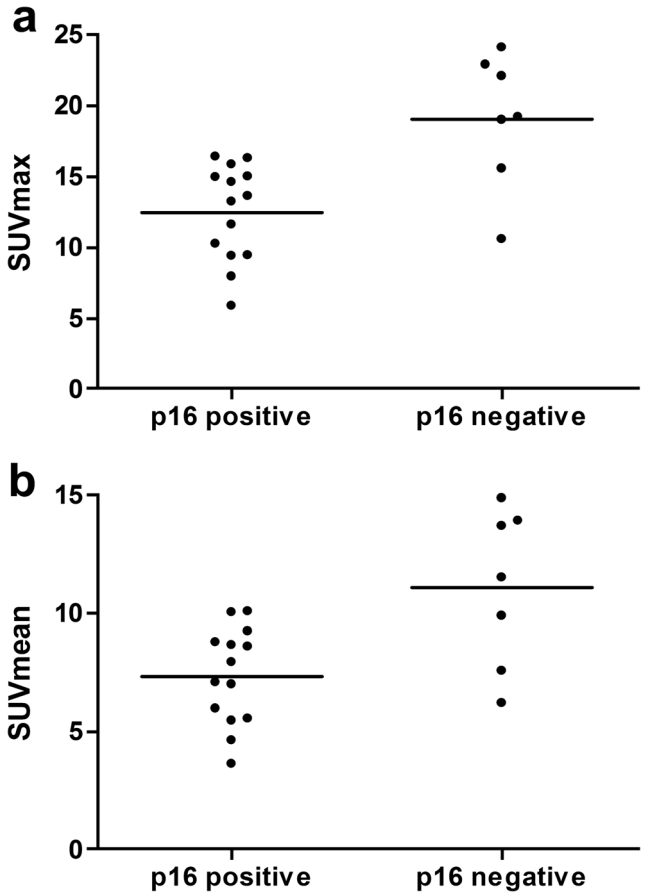

Fig. 3 Comparison of SUV values between p16-positive and p16-negative tumors. **a** SUV_{max} values of p16-negative tumors are statistically significant higher than those of p16-positive lesions (19.07 ± 4.70 *vs* 12.48 ± 3.38, $P = 0.006$). **b** SUV_{mean} values of p16-negative tumors are statistically significant higher than those of p16-positive lesions (11.10 ± 3.34 *vs* 7.33 ± 2.04, $P = 0.002$).

imaging, in particular, PET parameters can reflect histopathological features of HNSCC, is very important.

Previously, some studies also analyzed relationships between FDG-PET and histopathology in HNSCC. Overall, there were few reports [4, 16, 18–20]. Furthermore, the reported data were inconclusive. For instance, Yokobori et al. showed that SUV_{max} correlated statistically significant with microvessel density ($p = 0.407$, $P = 0.038$) and L-type amino acid transporter 1 (LAT1) ($p = 0.465$, $P = 0.018$), but not with expression of glucose transporter 1 (GLUT1) ($p = 0.167$, $P = 0.395$) or KI 67 ($p = 0.37$, $P = 0.060$) [33]. Also Grönroos et al. identified no significant correlations between SUV and GLUT 1 or KI 67 [18]. However, in the study of Deron, SUV_{max} correlated significantly with GLUT 1 ($r = 0.408$, $P = 0.04$) [34]. Furthermore, according to Jacob et al., SUV_{max} correlated well with KI 67 ($r = 0.78$) and another proliferation marker, namely PCNA (proliferating cell nuclear antigen), $r = 0.66$ [35]. In addition, Jacob et al. also identified that SUV_{max} correlated with tumor aggressiveness parameters DNA aneuploidy (2c deviation index) with a Pearson's correlation coefficient of 0.76 [35]. Similar controversial results were reported for associations of [^{18}F]FDG-PET parameters with other biomarkers like tumor suppressor protein p53 and hypoxia-inducible factor (HIF)-1α [16, 18, 36]. According to Grönroos et al., SUV_{max} tended to correlate with p53 ($p = 0.47$, $P = 0.078$) [18]. However, Rasmussen et al. could not identify significant correlations between SUV values and expression of p53 ($p = -0.42$, $P = 0.69$) [16]. Furthermore, according to Zhao et al., SUV_{max} correlated well with expression of HIF-1α [19]. Other authors did not confirm this result [18]. It is unknown, why some authors found significant correlations between PET and histopathological parameters in HNSCC while others did not.

Based on our previous data [37], we hypothesized that well, moderately, and poorly differentiated tumors might show also different relationships of [^{18}F]FDG-PET parameters and histopathology. For instance, previously, we found that associations between imaging parameters, such as SUV and apparent diffusion coefficient, depended significantly on tumor grading [37]. The present study confirmed our assumption. In the overall sample, no significant correlations were found between the analyzed PET and histopathological parameters. This finding may suggest that there are no associations between PET and histopathology. However, separate correlation analyses in the subgroups based on tumor grading revealed other results. As seen, in G1/2 carcinomas, there were also no significant correlations between the investigated parameters. Only HIF-1α tended to correlate with SUV_{max} and SUV_{mean}. However, in G3 tumors, SUV_{max} and SUV_{mean} correlated statistical significant with cell count. It is unclear why tumor grading influences the relationships between PET values and histopathology. To the best of our knowledge, this phenomenon has not been described previously. The exact cause of this finding is unclear. Obviously, different tumor architectures show also different associations between metabolic activity and morphological features. Presumably, one or more histopathological factors, which are incorporated into grading system in HNSCC, like cell size, nuclear pleomorphism, number of mitoses, pattern of invasion, and presence or absence of inflammatory infiltrates may play a role here. Furthermore, this finding may be related to the fact that high-grade tumors have other relations between parenchyma and stroma than low-grade lesion [38, 39]. In addition, poorly differentiated carcinomas have also higher microvascular density in comparison to low/moderate HNSCC [38].

Our finding is very interesting and may explain controversial results of the previous studies. Presumably, they might contain well, moderately, and poorly differentiated tumors in several proportions. Consequently, this may induce different relationships between [^{18}F]FDG-PET and histopathological parameters. In addition, our findings suggest that [^{18}F]FDG-PET parameters can be used as

Table 3. Correlations between SUV values and histopathological features

Parameters	EGFR	VEGF	Hif1alpha	P53	Ki 67	Cell count
Overall sample ($n = 22$)						
SUV_{max}	$\rho = 0.04$	$\rho = 0.30$	$\rho = -0.06$	$\rho = -0.07$	$\rho = 0.01$	$\rho = 0.22$
	$P = 0.85$	$P = 0.19$	$P = 0.78$	$P = 0.78$	$P = 0.96$	$P = 0.33$
SUV_{mean}	$\rho = 0.15$	$\rho = 0.23$	$\rho = 0.01$	$\rho = 0.05$	$\rho = 0.02$	$\rho = 0.13$
	$P = 0.54$	$P = 0.32$	$P = 0.95$	$P = 0.83$	$P = 0.92$	$P = 0.58$
G 1/2 tumors ($n = 10$)						
SUV_{max}	$\rho = -0.127$	$\rho = 0.418$	$\rho = -0.624$	$\rho = 0.152$	$\rho = 0.031$	$\rho = 0.091$
	$P = 0.726$	$P = 0.229$	$P = 0.054$	$P = 0.676$	$P = 0.933$	$P = 0.803$
SUV_{mean}	$\rho = 0.079$	$\rho = 0.176$	$\rho = -0.564$	$\rho = 0.273$	$\rho = 0.055$	$\rho = -0.200$
	$P = 0.829$	$P = 0.627$	$P = 0.09$	$P = 0.446$	$P = 0.880$	$P = 0.580$
G 3 tumors ($n = 12$)						
SUV_{max}	$\rho = 0.245$	$\rho = 0.353$	$\rho = -0.127$	$\rho = 0.045$	$\rho = 0.028$	*$\rho = 0.580$*
	$P = 0.467$	$P = 0.287$	$P = 0.709$	$P = 0.894$	$P = 0.931$	*$P = 0.048$*
SUV_{mean}	$\rho = 0.227$	$\rho = 0.381$	$\rho = -0.227$	$\rho = 0.027$	$\rho = 0.029$	*$\rho = 0.587$*
	$P = 0.502$	$P = 0.247$	$P = 0.502$	$P = 0.937$	$P = 0.930$	*$P = 0.045$*

Significant correlations are highlighted in italics

surrogate cellularity marker in poorly differentiated HNSCC but not in well/moderately differentiated tumors.

Furthermore, we found that p16-negative tumors showed statistically significant higher SUV_{max} and SUV_{mean} values than p16-positive carcinomas. This finding is in agreement with those of Rasmussen [16]. According to the literature, p16-positive tumors are smaller and less FDG avid than HPV-negative tumors [40]. Furthermore, p16 positivity has been reported to be associated with the most favorable prognosis [16, 40]. Therefore, our finding seems to be logical.

Our study is limited due to a small number of patients. Furthermore, the histopathological samples only represent a relatively small portion of the tumors, whereas the FDG-PET parameters were analyzed as a whole tumor measurement. Clearly, further investigations with more cases are needed to verify our results.

In conclusion, associations between [^{18}F]FDG-PET parameters and different histopathological features in HNSCC depend significantly on tumor grading. In G1/2 carcinomas, there were no significant correlations between [^{18}F]FDG-PET parameters and histopathology. In G3 lesions, SUV_{max} and SUV_{mean} reflect tumor cellularity.

Authors' Contributions. AS drafted the manuscript and participated in the design of the study. HJM participated in the design of the study and coordination and participated in the histopathological analyses. AKH performed the histopathological analyses. KW performed the statistical analysis. OS participated in the design of the study and coordination. SP participated in the design of the study and helped to draft the manuscript. All authors read and approved the final manuscript.

Compliance with Ethical Standards

Ethics Approval and Consent to Participate

This prospective study was approved by the institutional review board (Ethic Committee of the Medical Faculty, University of Leipzig) and all patients gave written informed consent. All procedures performed in the present study involving human participants were in accordance with the ethical standards of the institutional and/or national research committee and with the 1964 Helsinki declaration and its later amendments or comparable ethical standards.

Consent for Publication

Consent for publication is not applicable for this study.

Availability of Data and Material

Conflict of Interest

The authors declare that they have no conflict of interest.

References

1. Braakhuis BJ, Leemans CR, Visser O (2014) Incidence and survival trends of head and neck squamous cell carcinoma in the Netherlands between 1989 and 2011. Oral Oncol 50:670–675
2. Adams S, Baum RP, Stuckensen T, Bitter K, Hör G (1998) Prospective comparison of ^{18}F-FDG PET with conventional imaging modalities (CT, MRI, US) in lymph node staging of head and neck cancer. Eur J Nucl Med 25:1255–1260
3. Ng SH, Yen TC, Liao CT, Chang JT, Chan SC, Ko SF, Wang HM, Wong HF (2005) 18F-FDG PET and CT/MRI in oral cavity squamous cell carcinoma: a prospective study of 124 patients with histologic correlation. J Nucl Med 46:1136–1143
4. Surov A, Stumpp P, Meyer HJ, Gawlitza M, Höhn AK, Boehm A, Sabri O, Kahn T, Purz S (2016) Simultaneous 18F-FDG-PET/MRI: associations between diffusion, glucose metabolism and histopathological parameters in patients with head and neck squamous cell carcinoma. Oral Oncol 58:14–20
5. Varoquaux A, Rager O, Poncet A, Delattre BMA, Ratib O, Becker CD, Dulguerov P, Dulguerov N, Zaidi H, Becker M (2014) Detection and quantification of focal uptake in head and neck tumours: ^{18}F-FDG PET/MR versus PET/CT. Eur J Nucl Med Mol Imaging 41:462–475
6. Goel R, Moore W, Sumer B, Khan S, Sher D, Subramaniam RM (2017) Clinical practice in PET/CT for the Management of Head and Neck Squamous Cell Cancer. AJR Am J Roentgenol 209:289–303
7. Chan SC, Cheng NM, Hsieh CH, Ng SH, Lin CY, Yen TC, Hsu CL, Wan HM, Liao CT, Chang KP, Wang JJ (2017) Multiparametric imaging using ^{18}F-FDG PET/CT heterogeneity parameters and functional MRI techniques: prognostic significance in patients with primary advanced oropharyngeal or hypopharyngeal squamous cell carcinoma treated with chemoradiotherapy. Oncotarget 8:62606–62621

8. Ryu IS, Roh JL, Kim JS, Lee JH, Cho KJ, Choi SH, Nam SY, Kim SY (2016) Impact of ^{18}F -FDG PET/CT staging on management and prognostic stratification in head and neck squamous cell carcinoma: a prospective observational study. Eur J Cancer 63:88–96
9. Haerle SK, Huber GF, Hany TF, Ahmad N, Schmid DT (2010) Is there a correlation between ^{18}F-FDG-PET standardized uptake value, T-classification, histological grading and the anatomic subsites in newly diagnosed squamous cell carcinoma of the head and neck? Eur Arch Otorhinolaryngol 267:1635–1640
10. Kendi AT, Corey A, Magliocca KR, Nickleach DC, Galt J, Switchenko JM, el-Deiry MW, Wadsworth JT, Hudgins PA, Saba NF, Schuster DM (2015) ^{18}F-FDG-PET/CT parameters as imaging biomarkers in oral cavity squamous cell carcinoma, is visual analysis of PET and contrast enhanced CT better than the numbers? Eur J Radiol 84:1171–1176
11. Li SJ, Guo W, Ren GX, Huang G, Chen T, Song SL (2008) Expression of Glut-1 in primary and recurrent head and neck squamous cell carcinomas, and compared with 2-[^{18}F]fluoro-2-deoxy-D-glucose accumulation in positron emission tomography. Br J Oral Maxillofac Surg 46:180–186
12. Abgral R, Keromnes N, Robin P, le Roux PY, Bourhis D, Palard X, Rousset J, Valette G, Marianowski R, Salaün PY (2014) Prognostic value of volumetric parameters measured by ^{18}F-FDG PET/CT in patients with head and neck squamous cell carcinoma. Eur J Nucl Med Mol Imaging 41:659–667
13. Kim SY, Roh JL, Kim JS, Ryu CH, Lee JH, Cho KJ, Choi SH, Nam SY (2008) Utility of FDG PET in patients with squamous cell carcinomas of the oral cavity. Eur J Surg Oncol 34:208–215
14. Kitagawa Y, Sano K, Nishizawa S, Nakamura M, Ogasawara T, Sadato N, Yonekura Y (2003) FDG-PET for prediction of tumour aggressiveness and response to intra-arterial chemotherapy and radiotherapy in head and neck cancer. Eur J Nucl Med Mol Imaging 30:63–71
15. Wong KH, Panek R, Welsh L, Mcquaid D, Dunlop A, Riddell A, Murray I, du Y, Chua S, Koh DM, Bhide S, Nutting C, Oyen WJG, Harrington K, Newbold KL (2016) The predictive value of early assessment after 1 cycle of induction chemotherapy with 18F-FDG PET/CT and diffusion-weighted MRI for response to radical chemo-radiotherapy in head and neck squamous cell carcinoma. J Nucl Med 57:1843–1850
16. Rasmussen GB, Vogelius IR, Rasmussen JH, Schumaker L, Ioffe O, Cullen K, Fischer BM, Therkildsen MH, Specht L, Bentzen SM (2015) Immunohistochemical biomarkers and FDG uptake on PET/CT in head and neck squamous cell carcinoma. Acta Oncol 54:1408–1415
17. Troy JD, Weissfeld JL, Youk AO, Thomas S, Wang L, Grandis JR (2013) Expression of EGFR, VEGF, and NOTCH1 suggest differences in tumor angiogenesis in HPV-positive and HPV-negative head and neck squamous cell carcinoma. Head Neck Pathol 7:344–355
18. Grönroos TJ, Lehtiö K, Söderström KO, Kronqvist P, Laine J, Eskola O, Viljanen T, Grénman R, Solin O, Minn H (2014) Hypoxia, blood flow and metabolism in squamous-cell carcinoma of the head and neck: correlations between multiple immunohistochemical parameters and PET. BMC Cancer 14:876
19. Zhao K, Yang SY, Zhou SH et al (2014) Fluorodeoxyglucose uptake in laryngeal carcinoma is associated with the expression of glucose transporter 1 and hypoxia inducible factor 1α and the phosphoinositide 3 kinase/protein kinase B pathway. Oncol Lett 7:984–990
20. Han MW, Lee HJ, Cho KJ, Kim JS, Roh JL, Choi SH, Nam SY, Kim SY (2012) Role of FDG-PET as a biological marker for predicting the hypoxic status of tongue cancer. Head Neck 34:1395–1402
21. Surov A, Gottschling S, Mawrin C, Prell J, Spielmann RP, Wienke A, Fiedler E (2015) Diffusion weighted imaging in meningioma: prediction of tumor grade and association with histopathological parameters. Transl Oncol 8:517–523
22. Surov A, Caysa H, Wienke A, Spielmann RP, Fiedler E (2015) Correlation between different ADC fractions, cell count, Ki-67, total nucleic areas and average nucleic areas in meningothelial meningiomas. Anticancer Res 35:6841–6846
23. Doll CM, Moughan J, Klimowicz A, Ho CK, Kornaga EN, Lees-Miller SP, Ajani JA, Crane CH, Kachnic LA, Okawara GS, Berk LB, Roof KS, Becker MJ, Grisell DL, Ellis RJ, Sperduto PW, Marsa GW, Guha C, Magliocco AM (2017) Significance of co-expression of epidermal growth factor receptor and Ki67 on clinical outcome in patients with anal cancer treated with chemoradiotherapy: an analysis of NRG oncology RTOG 9811. Int J Radiat Oncol Biol Phys 97:554–562
24. Almangush A, Heikkinen I, Mäkitie AA, Coletta RD, Läärä E, Leivo I, Salo T (2017) Prognostic biomarkers for oral tongue squamous cell carcinoma: a systematic review and meta-analysis. Br J Cancer 117:856–866
25. Gioacchini FM, Alicandri-Ciufelli M, Magliulo G, Rubini C, Presutti L, Re M (2015) The clinical relevance of Ki-67 expression in laryngeal squamous cell carcinoma. Eur Arch Otorhinolaryngol 272:1569–1576
26. Oliveira LR, Ribeiro-Silva A (2011) Prognostic significance of immunohistochemical biomarkers in oral squamous cell carcinoma. Int J Oral Maxillofac Surg 40:298–307
27. Bossi P, Resteghini C, Paielli N, Licitra L, Pilotti S, Perrone F (2016) Prognostic and predictive value of EGFR in head and neck squamous cell carcinoma. Oncotarget 7:74362–74379
28. Ma X, Huang J, Wu X, Li X, Zhang J, Xue L, Li P, Liu L (2014) Epidermal growth factor receptor could play a prognostic role to predict the outcome of nasopharyngeal carcinoma: a meta-analysis. Cancer Biomark 14:267–277
29. Tandon S, Tudur-Smith C, Riley RD, Boyd MT, Jones TM (2010) A systematic review of p53 as a prognostic factor of survival in squamous cell carcinoma of the four main anatomical subsites of the head and neck. Cancer Epidemiol Biomark Prev 19:574–587
30. Zang J, Li C, Zhao LN, Shi M, Zhou YC, Wang JH, Li X (2013) Prognostic value of vascular endothelial growth factor in patients with head and neck cancer: a meta-analysis. Head Neck 35:1507–1514
31. Melkane AE, Auperin A, Saulnier P, Lacroix L, Vielh P, Casiraghi O, Msakni I, Drusch F, Temam S (2014) Human papillomavirus prevalence and prognostic implication in oropharyngeal squamous cell carcinomas. Head Neck 36:257–265
32. Gong L, Zhang W, Zhou J, Lu J, Xiong H, Shi X, Chen J (2013) Prognostic value of HIFs expression in head and neck cancer: a systematic review. PLoS ON 8:e75094
33. Yokobori Y, Toyoda M, Sakakura K, Kaira K, Tsushima Y, Chikamatsu K (2015) ^{18}F-FDG uptake on PET correlates with biological potential in early oral squamous cell carcinoma. Acta Otolaryngol 135:494–499
34. Deron P, Vangestel C, Goethals I, de Potter A, Peeters M, Vermeersch H, van de Wiele C (2011) FDG uptake in primary squamous cellcarcinoma of the head and neck. The relationship between over expression of glucose transporters and hexokinases, tumour proliferation and apoptosis. Nuklearmedizin 50:15–21
35. Jacob R, Welkoborsky HJ, Mann WJ, Jauch M, Amedee R (2001) [Fluorine-18] Fluorodeoxyglucose positron emission tomography, DNA ploidy and growth fraction in squamous-cell carcinomas of the head and neck. ORL 63:307–313
36. Norikane T, Yamamoto Y, Maeda Y, Kudomi N, Matsunaga T, Haba R, Iwasaki A, Hoshikawa H, Nishiyama Y (2014) Correlation of (18)F-fluoromisonidazole PET findings with HIF-1α and p53 expressions in head and neck cancer: comparison with ^{18}F-FDG PET. Nucl Med Commun 35:30–35
37. Leifels L, Purz S, Stumpp P, Schob S, Meyer HJ, Kahn T, Sabri O, Surov A (2017) Associations between 18F-FDG-PET, DWI, and DCE parameters in patients with head and neck squamous cell carcinoma depend on tumor grading. Contrast Media Mol Imaging 5369625
38. Wadhwan V, Sharma P, Saxena C et al (2015) Grading angiogenesis in oral squamous cell carcinoma: a histomorphometric study. Indian J Dent Res 26:26–30
39. Anneroth G, Hansen LS (1984) A methodologic study of histologic classification and grading of malignancy in oral squamous cell carcinoma. Scand J Dent Res 92:448–468
40. Schouten CS, Hakim S, Boellaard R, Bloemena E, Doornaert PA, Witte BI, Braakhuis BJM, Brakenhoff RH, Leemans CR, Hoekstra OS, de Bree R (2016) Interaction of quantitative ^{18}F-FDG-PET-CT imaging parameters and human papillomavirus status in oropharyngeal squamous cell carcinoma. Head Neck 38:529–535